THE JOURNAL OF BIOLOGICAL CHEMISTRY VOL. 283, NO. 26, pp. 18323–18330, June 27, 2008
Printed in the U.S.A.

Rab35 and Its GAP EPI64C in T Cells Regulate Receptor Recycling and Immunological Synapse Formation*[S]

Received for publication, January 3, 2008, and in revised form, April 11, 2008 Published, JBC Papers in Press, April 30, 2008, DOI 10.1074/jbc.M800056200

Genaro Patino-Lopez[‡1], Xiaoyun Dong[‡1], Khadija Ben-Aissa[‡], Kelsie M. Bernot[§], Takashi Itoh[¶‖], Mitsunori Fukuda[¶‖], Michael J. Kruhlak[‡], Lawrence E. Samelson[§], and Stephen Shaw[‡2]

From the [‡]Experimental Immunology Branch and [§]Laboratory of Cellular and Molecular Biology, NCI, National Institutes of Health, Bethesda, Maryland 20892, [¶]Fukuda Initiative Research Unit, RIKEN (The Institute of Physical and Chemical Research), 2-1 Hirosawa, Wako, Saitama 351-0198, and the [‖]Laboratory of Membrane Trafficking Mechanisms, Department of Developmental Biology and Neurosciences, Graduate School of Life Sciences, Tohoku University, Aobayama, Aoba-ku, Sendai, Miyagi 980-8578, Japan

Upon antigen recognition, T-cell receptor (TCR/CD3) and other signaling molecules become enriched in a specialized contact site between the T cell and antigen-presenting cell, *i.e.* the immunological synapse (IS). Enrichment occurs via mechanisms that include polarized secretion from recycling endosomes, but the Rabs and RabGAPs that regulate this are unknown. EPI64C (TBC1D10C) is an uncharacterized candidate RabGAP we identified by mass spectrometry as abundant in human peripheral blood T cells that is preferentially expressed in hematopoietic cells. EPI64C is a Rab35-GAP based both on *in vitro* Rab35-specific GAP activity and findings in transfection assays. EPI64C and Rab35 dominant negative (DN) constructs each impaired transferrin export from a recycling pathway in Jurkat T-cells and induced large vacuoles marked by transferrin receptor, TCR, and SNAREs implicated in TCR-polarized secretion. Rab35 localized to the plasma membrane and to intracellular vesicles where it substantially colocalized with TfR and with TCR. Rab35 was strongly recruited to the IS. Conjugate formation was impaired by transfection with Rab35-DN or EPI64C and by EPI64C knock down. TCR enrichment at the IS was impaired by Rab35-DN. Thus, EPI64C and Rab35 regulate a recycling pathway in T cells and contribute to IS formation, most likely by participating in TCR transport to the IS.

The immunological synapse (IS)[3] is a specialized contact between T lymphocytes and antigen-presenting cells (APC) into which accumulate T-cell antigen receptor (TCR), coreceptors, and signaling and cytoskeletal components (1–7). Enrichment of proteins in the IS occurs in part by diffusion and retention at the contact region (*i.e.*"mutual co-capping") (8, 9). Furthermore, submembranous flow of the actomyosin cortex contributes to molecular concentration in the IS (10, 11). Recent data indicate that polarized exocytosis from a rapid recycling pathway is particularly important for the enrichment of some synapse components, including TCR (12–16).

Rab proteins are major intracellular transport regulators in eukaryotes; they function in vesicle formation, motility, docking, and fusion (17, 18). Over 60 mammalian Rab proteins have been identified, and each is thought to regulate distinct intracellular transport steps through its temporal and spatial association with various interacting proteins. Guanine exchange factors and GTPase-activating proteins (GAPs) control the switch between active GTP-bound and inactive GDP-bound Rab proteins. Although the TBC (Tre/Bub2/Cdc16) domain is a hallmark of RabGAPs (19), few of the more than 50 putative TBC domain-containing proteins present in the human genome have been paired with their target Rab. One recent notable success was identification of EPI64 (EBP50-PDZ interactor of 64kD) as a GAP specific for Rab27a (20).

EPI64 is a broadly expressed TBC domain-containing protein first identified in placental microvilli (21). Recent studies have implicated it in regulating microvillus architecture (22). EPI64 has two paralogs in mouse and human. One of these, EPI64B (FLJ13130/Rab27-GAP β) is quite similar to EPI64 (81% identity in the TBC domain) and shares Rab27a GAP activity (20). The other, EPI64C (mFLJ00332), is more divergent (only 60% identity in the TBC domain) and lacks the capacity to regulate Rab27a in melanocytes. Our studies identified this divergent member, EPI64C, in hematopoietic cells and especially primary T cells and demonstrate that EPI64C is a GAP for Rab35. EPI64C and Rab35 both regulate transferrin receptor (TfR) recycling in Jurkat cells, as was recently shown for Rab35 in HeLa cells (23). Moreover, colocalization analysis, transfection studies, and knock down show that together EPI64 and Rab35 facilitate conjugate formation between T cells and APC in a manner indicative of regulating polarized secretion from recycling endosomes.

EXPERIMENTAL PROCEDURES

Antibodies, Reagents, Cells, and Replication—Anti-Rab35 antibody (23) was kindly provided by Dr. Arnaud Echard (Institut Curie, Paris), rabbit anti-EPI64C antibody raised against

* This work was supported, in whole or in part, by the National Institutes of Health NCI Intramural Research Program. The costs of publication of this article were defrayed in part by the payment of page charges. This article must therefore be hereby marked "*advertisement*" in accordance with 18 U.S.C. Section 1734 solely to indicate this fact.

[S] The on-line version of this article (available at http://www.jbc.org) contains supplemental Figs. S1–S8 and a movie.

[1] Both authors contributed equally to this work.

[2] To whom correspondence should be addressed: National Institutes of Health, Bldg. 10, Rm. 4B36, 10 Center Dr., MSC 1360, Bethesda, MD 20892-1360. Tel.: 301-435-6499; Fax: 301-496-0887; E-mail: sshaw@nih.gov.

[3] The abbreviations used are: IS, immunological synapse; APC, antigen-presenting cell; DN, dominant negative; GAP, GTPase-activating protein; GFP, green fluorescent protein; SEE, staphylococcus enterotoxin E; SNARE, soluble NSF attachment protein receptor; TBC, Tre/Bub2/Cdc16; TCR, T-cell receptor; TfR, transferrin receptor; mRFP, monomeric red fluorescent protein.

amino acids 25–39 of human EPI64C (DSELSGPGPYRQADR), anti-EEA1, anti-LAMP-2, anti-calnexin, and anti-TfR were provided by Dr. Paul Roche (NCI, National Institutes of Health, Bethesda, MD), anti-α-tubulin antibody was from Sigma-Aldrich, and anti-CD3 monoclonal CD3-4B5 was kindly provided by Dr. Walter Knapp, Institute fur Immunologie, Vienna. Other antibodies were Alexa Fluor 546 phalloidin, goat anti-mouse IgG-Alexa 647, and Alexa 488 (Invitrogen) and goat anti-mouse IRDye 680 and goat anti-rabbit IRDye 800CW (LI-COR, Lincoln, NE). Other reagents were lucifer yellow (Sigma), staphylococcus enterotoxin E (SEE) (Toxin Technology, Sarasota, FL), and CellTracker Blue and Vybrant CFDA S.E. (Invitrogen). Jurkat Tag cells were kindly provided by Dr. Gerald Crabtree (Stanford University); Raji B-lymphoma cells and human embryonic kidney 293 cells were from ATCC (Manassas, VA). Primary human T lymphocytes were isolated from the blood of healthy human volunteers by leukapheresis and elutriation or immunomagnetic negative selection (24, 25). Unless otherwise indicated, all results shown are representative of at least three independent experiments.

Plasmid Constructs—Human EPI64C, Rab5a, 5b, 5c, 6a, 6b, 7, 8a, 8b, 9b, 10, 11a, 11b, 14, 21, 27a, 35, TCR-ζ, Vamp3, SNAP3, and syntaxin4 were amplified from Jurkat Tag RNA (RNAeasy Mini kit; Qiagen, Inc.) by reverse transcription PCR (SuperScript One-Step RT-PCR for Long Templates; Invitrogen) and cloned into pENTR vectors by recombination (pENTR/D-TOPO cloning kit; Invitrogen). EPI64C (R141K), Rab35 (S22N or Q67L), and Rab27a (T23N or Q78L) were generated using QuikChange site-directed mutagenesis (Stratagene); mutants were completely sequenced. Inserts were transferred from pENTR into Gateway destination vectors from the Protein Expression Laboratory (NCI-Frederick, National Institutes of Health, Frederick, MD) (pDest732 (N-terminal GFP tag), pDest733 (N-terminal monomeric red fluorescent protein (mRFP) tag), pDest472 (C-terminal GFP tag for TCR-ζ)) by an LR reaction according to the manufacturer's recommendations (Invitrogen) to construct mammalian expression vectors. The TCR-ζ chain was also subcloned into pEYFP-N1 (Clontech). Both pDest472 and pEYFP-N1 constructs were rendered monomeric by a published A206K substitution (26).

Western Blotting and Analysis—Cells were lysed in 1× NuPAGE LDS sample buffer (Invitrogen) containing 20 mM dithiothreitol (Sigma), sonicated three times for 10 s (Ultrasonic Processor GE130; Sonics & Materials, Inc., Newtown, CT), and heated at 70 °C for 7 min. Equal amounts of protein (45 μg) from each preparation were resolved by 4–12% SDS-NuPAGE gels, transferred to nitrocellulose membranes, and analyzed by Western blot using an Odyssey Infrared Imaging System (LI-COR Biosciences).

Conjugate Formation—Conjugate formation was determined by flow cytometry. Human Jurkat cells were transfected with plasmids encoding tagged proteins as indicated in each figure legend. The next day, Raji cells were loaded with 0.5 μM Cell Tracker carboxyfluorescein succinimidyl ester (Invitrogen) for 10 min at room temperature, pulsed for 15 min at 37 °C with 5 μg/ml SEE, and washed. Jurkat cells and Raji APCs were then mixed at a ratio of 1:1 (1.0×10^6 cells), centrifuged at $\sim 18 \times g$ for 10 s, and incubated for 30 min at 37 °C in 5 ml of polystyrene round-bottom tubes. Cells were fixed for 10 min with 2% paraformaldehyde. After gentle resuspension, cells were analyzed on FACSCalibur or FACS Vantage and data analyzed with Flowjo 7.2 (Tree Star, Inc., Ashland, OR). Conjugate formation was determined as the fraction of RFP+ events that were also carboxyfluorescein succinimidyl ester-positive. Statistical significance was assessed by one-tailed paired Student's *t* test. For imaging studies, Raji cells were stained with CellTracker Blue, and conjugates were formed in similar manner and analyzed by confocal microscopy as below.

Microscopy—Jurkat cells transfected with mRFP- and/or GFP-tagged plasmids were allowed to interact for 10 min with poly-lysine-precoated glass coverslips (MatTek Corporation, Ashland, MA) and then were either fixed for 10 min with 4% paraformaldehyde or permeabilized for 10 min with 0.1% Triton X-100; in some studies cells were also stained with mouse anti-α-tubulin antibody, followed by goat anti-mouse IgG-Alexa 647 (Invitrogen) at room temperature for 1 h or the culture medium was replaced with imaging medium (RPMI without phenol red, 10% fetal calf serum, 25 mM HEPES). The cells were imaged with a Zeiss LSM 510 META confocal microscope using a ×100 (N.A. 1.4) oil immersion objective lens (Zeiss, Thornwood, NY) or a Zeiss Axiovert 200 microscope equipped with a Perkin-Elmer Ultraview spinning disc confocal system. Images were captured with an Orca-ERII CCD camera (Hamamatsu). A hot air blower and an objective warmer were used to maintain live samples at 37 °C. Multicolor imaging was done using multitrack configuration (filters, laser power, and detector gain) that gives no detectable bleed-through between channels. For live imaging during IS formation Raji cells were pulsed with 2 μg/ml SEE for 15 min at 37 °C and plated on Lab Tek chambers in RPMI. For detection and quantification of TCR accumulation at the synapse, conjugates were fixed with 4% paraformaldehyde and stained with anti-CD3 and then goat anti-mouse IgG-Alexa 488 without detergent to detect surface receptors only. A Z-stack with 0.5 μM step size was acquired for each field with conjugates and quantitation performed using Metamorph v6.4 (Universal Imaging, Downingtown, PA). After selection of the optical slice with highest green fluorescence in the contact area, the mean green intensity was measured along the plasma membrane at the contact site and at a comparable area along the plasma membrane elsewhere in the cell (where practical, at the opposite pole). All visual scoring of microscopy results was done "blind" in the sense that the scoring observer did not know the identity of the constructs transfected. Statistical comparisons were carried out by the nonparametric Mann-Whitney test.

Purification of Glutathione S-Transferase-Rabs and in Vitro GAP Assay—Purification of glutathione *S*-transferase-Rab and glutathione *S*-transferase-EPI64C proteins and thrombin digestion were performed as described previously (27, 28). The GTP- loading protocol and the *in vitro* GAP assay were performed as described previously (29). In this study 200 pmol of Rab proteins and 5 pmol of EPI64C protein were used for the GAP assay.

RNA Interference—The following 20-nucleotide sequences were inserted into a cherry-small hairpin RNA suppression vector (30) to target human EPI64-C (A, 5′-CTGAGAGGACCAT-

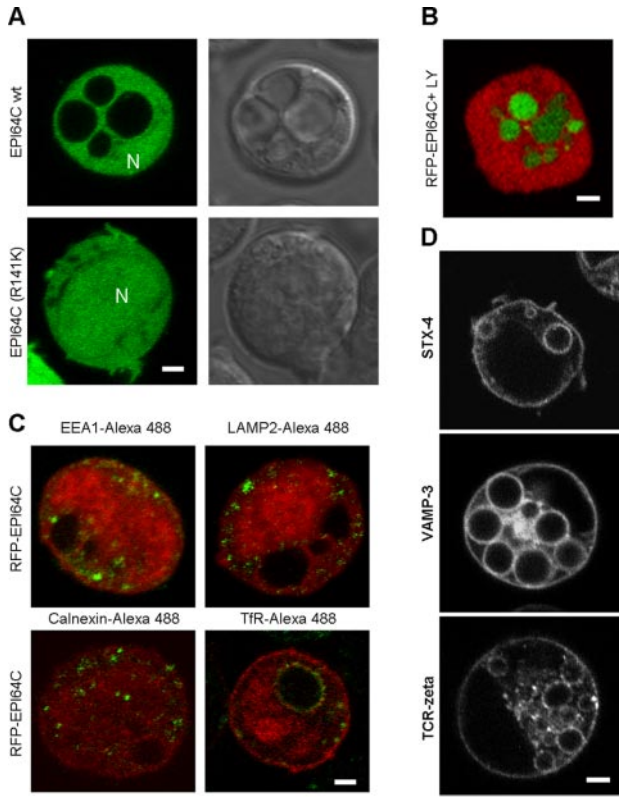

FIGURE 1. **EPI64C induces vesicles containing molecules related to synaptic TCR exocytosis.** *A*, expression of GFP-EPI64C wild type (*wt*) induces vacuoles in Jurkat cells seen by fluorescence and differential interference contrast, but the GAP-inactivated R141K mutant thereof does not. Images show representative cells 24 h after transfection. *N* indicates nucleus. *B*, lucifer yellow (4.0 mg/ml) was added to a suspension of mRFP-EPI64C-transfected cells. After 30 min cells were washed and imaged. *C*, Jurkat cells were transfected with mRFP-EPI64C and stained with anti-EEA1, anti-LAMP2, anti-calnexin, or anti-TfR, respectively. *D*, Jurkat cells were cotransfected with mRFP-EPI64C and plasmids encoding GFP-tagged proteins involved in synaptic TCR exocytosis: syntaxin4 (*Stx-4*), VAMP-3, or TCR-ζ. (Note that Stx-4 localizes not only to plasma membrane but also to endosomal membranes) (31). *Scale bars*, 2 μm.

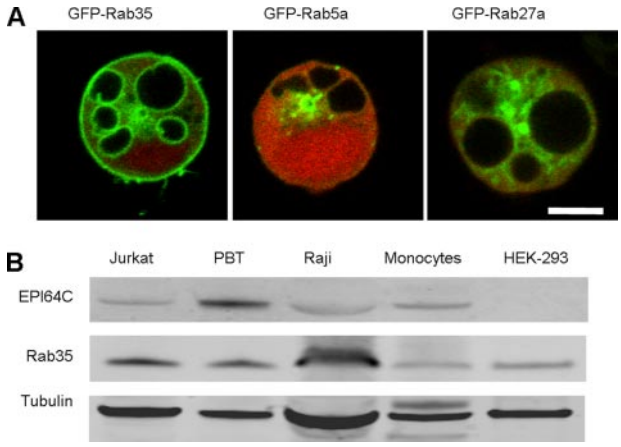

FIGURE 2. **EPI64C and Rab35 localization and expression.** *A*, Jurkat cells were co-transfected with mRFP-EPI64C and 16 different GFP-tagged Rab proteins. Rab35 was unique in the extent of enrichment on the EPI64C-induced vacuoles compared, for example, to Rab5a and Rab27a. *Scale bar*, 5 μm. *B*, Western blot analysis of EPI64C and Rab35 on lysates from a panel of hematopoietic cells and human embryonic kidney (*HEK*) 293 cells. PBT (peripheral blood T cells) and monocytes are from human blood; Raji is a human Burkitt lymphoma B-cell line.

GGACTTA-3′; B, 5′-GTACCAAAGCCAGCACCAAA-3′). Transient transfections in Jurkat were performed using 1×10^7 cells/sample along with 30–40 μg of plasmid DNA. Transfected Jurkat cells were used after 48–60 h for suppression.

Measurement of Transferrin Recycling—Transferrin recycling was done by preloading fluorescein isothiocyanate-tagged transferrin and determining the amount retained in cells after varying periods of incubation as described (23). The only differences were that: Jurkat cells in suspension were used rather than adherent HeLa cells; cells were 16 h post-transfection; and the medium used was RPMI rather than Dulbecco's modified Eagle's medium; and the mRFP tag was integral to the transfected constructs rather than co-transfected.

RESULTS

EPI64C Induces Vacuoles—After transfection into Jurkat cells, GFP-EPI64C was found distributed throughout the cell, including the nucleus (Fig. 1*A*). Many transfected cells (51% of 100 cells scored blind) developed one or more large (>1 μm) vacuoles visible both by their exclusion of GFP and by differential interference contrast imaging. This phenotype required GAP function because vacuoles were not observed in Jurkat cells transfected with a construct mutated at a TBC domain arginine critical for GAP activity (R141K). As controls, other TBC domain proteins (TBC1D15, AS160) were similarly transfected but did not cause formation of large vacuoles (supplemental Fig. S1).

To determine whether EPI64C vacuoles were components of an endocytic/recycling pathway, imaging was performed after addition of lucifer yellow to the culture medium. Within 30 min lucifer yellow was readily detectable in the large vacuoles (Fig. 1*B*). To characterize the vacuoles we stained with markers of key intracellular compartments. TfR receptor was strikingly localized to the vacuole membranes, indicating their involvement in a recycling pathway (Fig. 1*C*). In contrast, the markers of early endosomes (EEA1), lysosomes (LAMP2), and endoplasmic reticulum (calnexin) were not localized on the vacuole membrane but rather retained their normal pattern (Fig. 1*C* and supplemental Fig. S2).

In T cells there is a recycling pathway that mediates TCR externalization at the IS, whose molecular regulators remain to be fully characterized (13). We conjectured that our observation of EPI64C-mediated vacuole formation might be connected to that process. As an initial screen for this possibility, we investigated whether TCR or known molecular participants in synaptic TCR exocytosis would be present on these EPI64C-induced vacuoles (Fig. 1*D*). The results demonstrated that TCR-ζ and SNARE proteins implicated in synaptic TCR exocytosis (syntaxin4 and VAMP3) (13) were enriched on the surface of the vacuoles (Fig. 1*D* and supplemental Fig. S3).

EPI64C Vacuole Induction Is Mediated by Rab35 GAP Activity—To identify the Rab that EPI64C regulates to induce vacuole formation, we screened Rabs identified by proteomic profiling of peripheral blood T cells.[4] We hypothesized that the target Rab would localize to the EPI64C-induced vacuoles and therefore screened by co-transfection of the GFP-tagged Rab into Jurkat with mRFP-EPI64C. Of the 16 Rabs screened, Rab35

[4] J. J. Hao, G. Wang, T. Pisitkun, G. Patino-Lopez, M. A. Knepper, R. F. Shen, and S. Shaw (2007) submitted for publication.

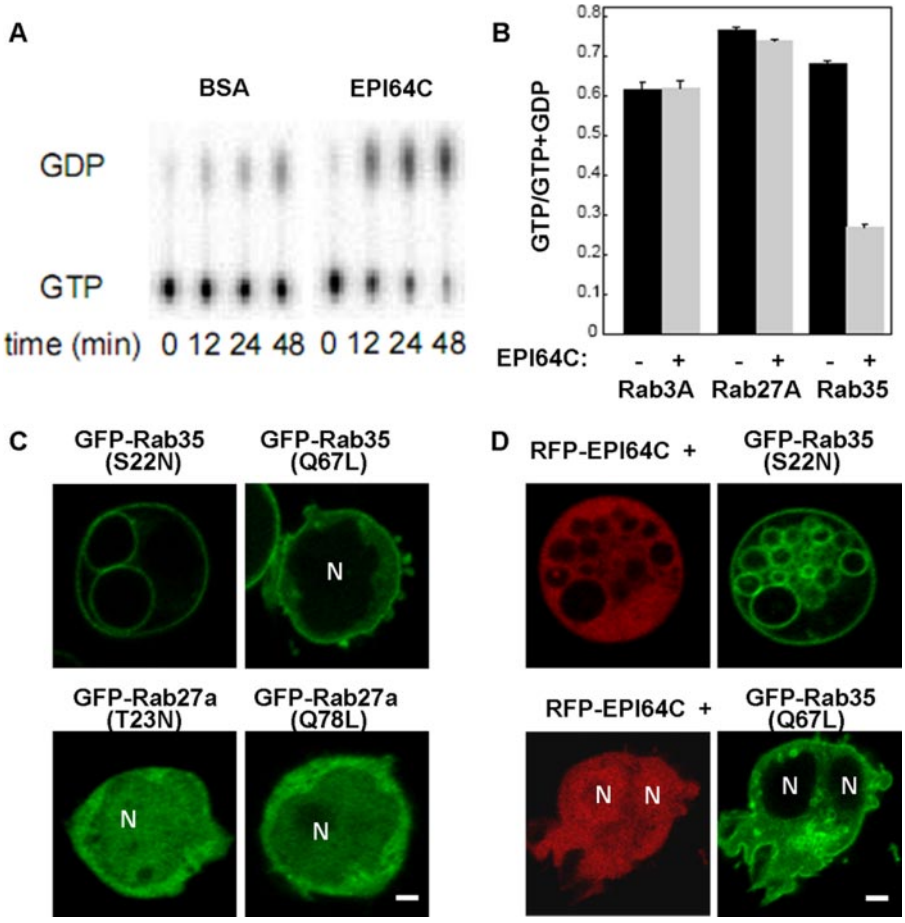

FIGURE 3. **EPI64C is a Rab35 GAP, *in vitro* and in-cell evidence.** EPI64C was analyzed for *in vitro* GAP activity on bacterially produced Rab35 and in-cell GAP activity. *A*, kinetic analysis. *B*, results of densitometric analysis expressed as the amount of the GTP-bound form of the indicated Rab after the reaction (Rab3a, 24 min; Rab27a, 48 min; and Rab35, 48 min) as a percentage of the amount before the reaction. *Error bars* represent the mean ± S.D. of data from three independent experiments. *C*, Jurkat cells were transfected with dominant negative constructs Rab35 (*S22N*) and Rab27a (*T23N*) and constitutive active constructs Rab35 (*Q67L*) and Rab27a (*Q78L*). Only Rab35 dominant negative induced large vacuoles. *D*, Jurkat cells were transfected with mRFP-EPI64C and Rab35-constitutive active (*Q67L*) or dominant negative (*S22N*) constructs. Only the constitutive active prevented EPI64C-induced vacuoles. *N* indicates nucleus. *Scale bars*, 2 μm.

was the one most strongly enriched on the vacuoles (Fig. 2*A*). Minimal enrichment on the vacuoles was seen with other Rabs (*e.g.* Fig. 2*A*, *Rab5a* and *Rab27a*).

Systematic microarray analysis available from SymAtlas had indicated that EPI64C expression occurs preferentially in hematopoietic cells whereas Rab35 is broadly expressed (32). Our analysis confirmed expression of EPI64C in the human hematopoietic cells tested and enrichment particularly in primary human peripheral blood T lymphocytes (Fig. 2*B*). Similar analysis of Rab35 expression confirmed its co-expression in lymphoid cells with EPI64C as well as in a non-hematopoietic kidney epithelial cell line.

To determine whether EPI64C functions as a Rab35 GAP, we measured its *in vitro* GAP activity for Rab35 (Fig. 3, *A* and *B*). The results showed that EPI64C is an efficient Rab35-GAP. The GAP activity of EPI64C is specific for Rab35 as it does not induce GTP hydrolysis by two other Rabs included as specificity controls, Rab3a or Rab27a.

The foregoing results can be explained by the hypothesis that EPI64C causes vacuoles in T cells by its Rab35-GAP activity that decreases intracellular Rab35-GTP. This hypothesis makes two testable predictions, both of which were experimentally confirmed. First, dominant negative (DN) Rab35 (S22N) caused vacuoles (of 50 cells scored, 70% had vacuoles >1.0 μm in diameter), but the control DN construct of Rab27a (T23N) did not (0% of 50 cells) (Fig. 3*C*). Second, constitutive active Rab35 (Q67L) blocked vacuole formation induced by EPI64C (0% of 50 cells had vacuoles), but the control constitutive active (Rab27a-Q78L) construct did not (Fig. 3*D*, and data not shown).

Furthermore, Rab35-DN impaired recycling of TfR back to the plasma membrane in Jurkat cells similar to its function in HeLa cells (23) (Fig. 4*A*). Notably, EPI64C overexpression also impaired this process. Thus, functional studies of Rab35 confirmed the two key predictions of the model that EPI64C mediates vacuole formation through its Rab35 GAP activity and analysis of transferrin recycling demonstrates that EPI64C regulates these Rab35-dependent events. In addition to inducing large vacuoles (Fig. 4*B*), transfection of GFP-Rab35-DN into Jurkat cells prominently highlighted smaller intracellular vesicles, reminding us of vesicles that transport both TCR and TfR (13). Staining of the transfected cells revealed extensive colocalization of Rab35-DN not only with TfR (Fig. 4*B*) but also with CD3 (Fig. 4*C*). This result suggested a role for Rab35 in trafficking of TCR as well as of TfR.

Rab35 and TCR Colocalize in Resting T Cells and at the IS—Localization of wild-type GFP-Rab35 in transfected Jurkat cells was analyzed. It localized both to plasma membrane and to intracellular vesicles, including the pericentriolar region (Fig. 5*A* and supplemental Fig. S4). Colocalization analysis showed TCR and Rab35 on solitary vesicles (Fig. 5*B* and supplemental Fig. S5) resembling those seen with anti-CD3 on Rab35-DN-transfected cells (Fig. 4*C*). TCR and Rab35 also colocalized in the pericentriolar region (Fig. 5*B*). The Rab35-positive vesicular compartment was also marked by VAMP3, the vSNARE that has been implicated in synaptic exocytosis (Fig. 5*C*). Thus, Rab35 marks a recycling compartment including both small solitary vacuoles and a major pericentrosomal accumulation where it colocalizes with TCR and thus has the potential to regulate synaptic TCR exocytosis.

We assessed Rab35 distribution during SEE superantigen-induced synapse formation between Jurkat T cells and Raji B

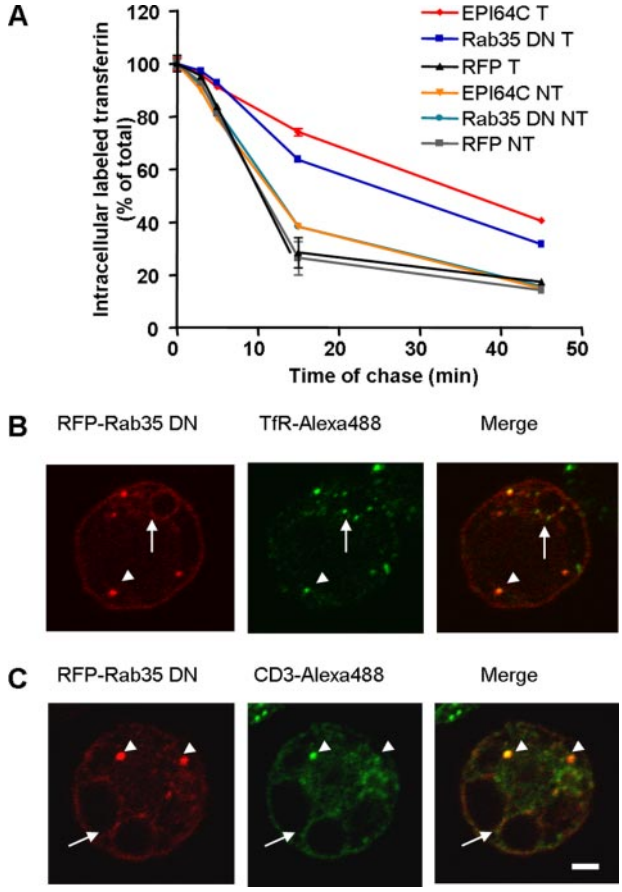

FIGURE 4. **EPI64C and Rab35 control receptor recycling.** *A*, EPI64-C and Rab35 DN control transferrin recycling. Jurkat cells transfected with mRFP-tagged EPI64-C, Rab35 DN, or mFRP were loaded with fluorescently labeled transferrin, and Tf recycling to the cell surface was quantified. Cells were gated on the transfected (*T*) or non-transfected (*NT*) cells in each population. EPI64C and Rab35DN caused slowdown of recycling compared with RFP and the NT cells from each treatment. Data shown are mean ± S.D. *B* and *C*, Jurkat cells were transfected with mRFP-Rab35DN (*red*) and after 16 h processed for immunofluorescence with anti-TfR (*B*) or anti-CD3-ϵ (*C*) (*green*). Rab35DN colocalized with both TfR and CD3 on vesicles (*arrowheads*) and vacuoles (*arrows*). *Scale bars*, 2 μm. Note some there is also some diffuse CD3 in ER that is not associated with TfR (38).

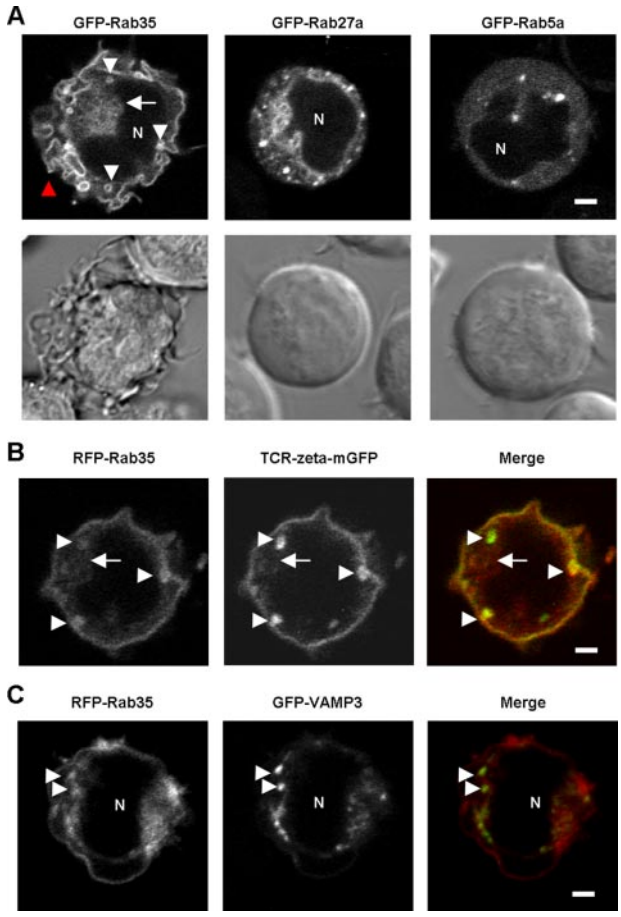

FIGURE 5. **Rab35 localization and colocalization with TCR.** Confocal images of Jurkat cells transfected with Rab35 alone or with other constructs. *A*, localization of GFP-Rab35 in transfected Jurkat cells compared with two other Rabs. *Arrow* highlights Rab35 localization in the pericentriolar region. *White arrowheads* highlight small vesicles enriched in Rab35, many of which are confirmed to be discontinuous with plasma membrane on serial sections. *Red arrowhead* highlights peripheral processes. *N* indicates nucleus. *B*, colocalization of TCR-ζ mGFP and mRFP-Rab35. *Arrows* highlight Rab35 and TCR-ζ in the pericentriolar region; *white arrowheads* highlight small vesicles enriched in Rab35 and TCR-ζ. *C*, GFP-VAMP3 is localized on many of the Rab35-positive granules (*arrowheads*) in co-transfected Jurkat cells. *N* indicates nucleus. *Scale bars*, 2 μm.

cell APCs (Fig. 6*A*). In the absence of SEE, Rab35 was evenly distributed on the T-cell surface, even at the site of contact with APCs. However, in the presence of SEE an expanded region of contact formed between T cell and APC into which Rab35 was enriched. We investigated the relationship between TCR localization (determined by TCR-ζ-GFP or –yellow fluorescent protein) and Rab35 in the T-cell-APC conjugates. Live cell imaging revealed that Rab35 and TCR-ζ were highly colocalized at the synapse (Fig. 6*B*). Among cell duplexes of Jurkat cells and Raji cells in the presence of antigen, Rab35 and TCR were co-enriched at the contact region in 57%. Moreover, Rab35 accumulation at the synapse was temporally concordant with TCR-ζ (Fig. 6*C* and supplemental movie). In contrast, TCR-ζ and Rab35 were never observed enriched at the contact region (0%) in the absence of antigen. Moreover, other Rabs did not accumulate at the synapse (data not shown). In addition, the pericentrosomal accumulation of Rab35 and TCR was often observed close to the synapse as expected based on the reorientation of the microtubule-organizing center toward the synapse (Fig. 6*B*, *right panel*).

Rab35 and EPI64C Regulate T-cell Conjugate Formation—To define the functional relevance for EPI64C and Rab35, a flow cytometric assay of conjugate formation was used to determine quantitatively whether Rab35 or EPI64C constructs perturbed T-cell conjugate formation (Fig. 7*A*). Transfection with EPI64C significantly inhibited conjugate formation, but the GAP-defective EPI64C mutant R141K did not. Transfection with Rab35-S22N (dominant negative DN) blocked conjugates to the same extent as EPI64C, but transfection with the Rab35-constitutive active did not. This alteration was not due to decreased surface CD3 in the transfected cells (supplemental Fig. S6) or to a general impairment in adhesion (supplemental Fig. S7). The cell mixtures analyzed by flow were also examined by fluorescence microscopy. When Jurkat cells transfected with Rab35-DN were found in contact with Raji cells there was never strong enrichment of Rab35-DN at the interface. In contrast, Jurkat transfected with Rab35-Q67L (constitutive active "CA") consistently showed enrichment of Rab35 CA at the contact (similar to that observed with Rab35 wild type, Fig. 7*B*). Rab35

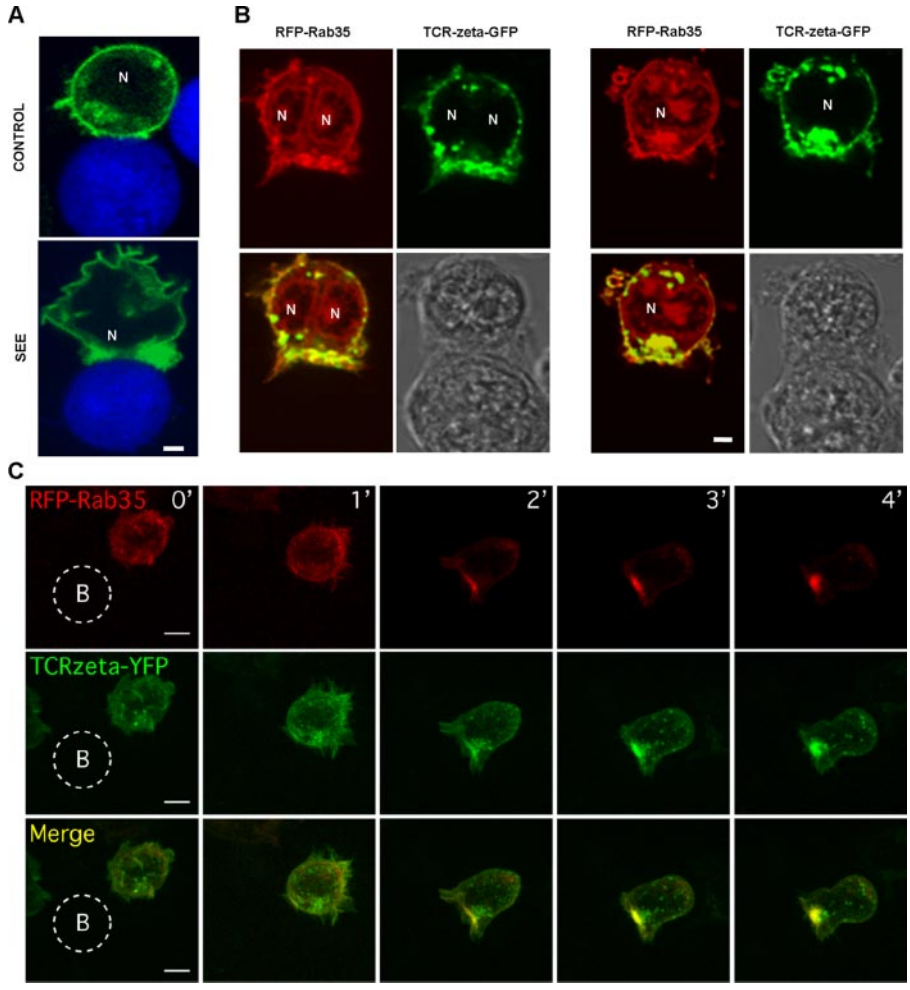

FIGURE 6. **Rab35 localizes to the IS.** Confocal images of Rab35-transfected Jurkat cells after incubation with Raji APCs in the absence or presence of superantigen SEE to stimulate conjugate formation. *A*, representative images of enhanced GFP-Rab35-transfected Jurkat cells in physical contact with Raji cells (stained with CellTracker Blue) with or without superantigen SEE. *B*, single color, merged, and differential interference contrast images of a representative conjugate between mRFP-Rab35 and TCR-ζ-GFP-transfected Jurkat cells and Raji cells in the presence of SEE. *N* indicates nucleus. *Scale bar*, 2 μm. *C*, transfected T cells were dropped onto SEE superantigen-pulsed Raji B cells (approximate location indicated by *dashed circle*). Maximum intensity projections from Z-stacks (17 slices, 1 μm apart) were compiled at the indicated time points. The zero time point represents the initiation of imaging, which was prior to the first contact between the T cell and the B cell. *Scale bar*, 5 μm. (Supplemental movie shows complete image set of maximum intensity projections from this observation).

was resistant to knockdown analysis because eight different constructs (of two different designs) failed to reduce its expression by more than 60%. However, knockdown analysis of EPI64C confirmed a role for it in conjugate formation (Fig. 7*C*). shEPI-B induced efficient knock down of protein expression and inhibited conjugate formation to about the same extent as its overexpression.

As a different approach to assess the effect of Rab35 DN on TCR accumulation at the IS, fixed non-permeabilized conjugates were stained with anti-TCR antibody to detect only surface-accessible TCR (13). Visual inspection of conjugates suggested that TCR was enriched at the IS in Rab35 DN-transfected cells but that the amount of enrichment was reduced. To quantitatively assess enrichment, TCR intensity in the synapse was compared with TCR intensity in the plasma membrane at the opposite pole of the cell in 25 randomly observed conjugates of each type (Fig. 7*D* and supplemental Fig. S8). The results demonstrate that Rab35 DN significantly impairs TCR enrichment in the synapse.

DISCUSSION

Rab35 was largely uncharacterized until a recent RNA interference screen for Rab protein function by Echard and coworkers revealed a role for it in cytokinesis (23). In doing so, they implicated Rab35 in control of a recycling pathway step that returns TfR receptor back to the plasma membrane. Our studies extend that understanding by identifying EPI64C as a Rab35-GAP that, like Rab35, regulates TfR recycling. Moreover, our studies demonstrate that Rab35 and its GAP EPI64C regulate formation of the IS.

We identify EPI64C as a Rab35-GAP based on multiple lines of evidence. *In vitro*, EPI64C has Rab35-selective GAP activity (Fig. 3, *A* and *B*). In cells, transfection with EPI64C mimics the effects of transfection with Rab35 DN. Both constructs impair recycling of TfR back to the plasma membrane (Fig. 4*A*), induce large vacuoles in Jurkat cells (Figs. 1*A* and 3*C*), and impair IS formation (Fig. 7*A*). Finally, in cells Rab35-constitutive active blocks the vacuole-inducing function of EPI64C (Fig. 3*D*).

The present study expands our understanding about RabGAPs. First, establishing EPI64C as a Rab35 GAP adds it to the handful of TBC domain proteins whose target GTPase(s) have been identified (20). In a recent systematic analysis, *in vitro* GAP assays indicate that Rab35 may have other GAPs, including EVI5, and possibly EPI64B (TBC1D10B) and TBC1D17 (33). Although our in-cell evidence does not confirm these putative Rab35 GAPs, others presumably exist because Rab35 is broadly expressed but EPI64C is selective to hematopoietic cells (Fig. 2 and SymAtlas). Second, our studies begin to flesh out concepts of RabGAPs in lymphocytes. We find only one report on that topic, which describes increased expression of AS160 in patients with atopic dermatitis (34). In addition to EPI64C, our mass spectrometric analysis[4] detected three other TBC domain proteins in lymphocytes: TBC1D15 (a Rab7 GAP) (35) and two uncharacterized ones (TBC1D24 and RUTBC1). The available data (SymAtlas and/or Unigene and Fig. 2*B*) suggest considerable tissue selectivity in expression of these GAPs in hematopoietic cells, consistent with special mechanisms for vesicular traffic in that lineage.

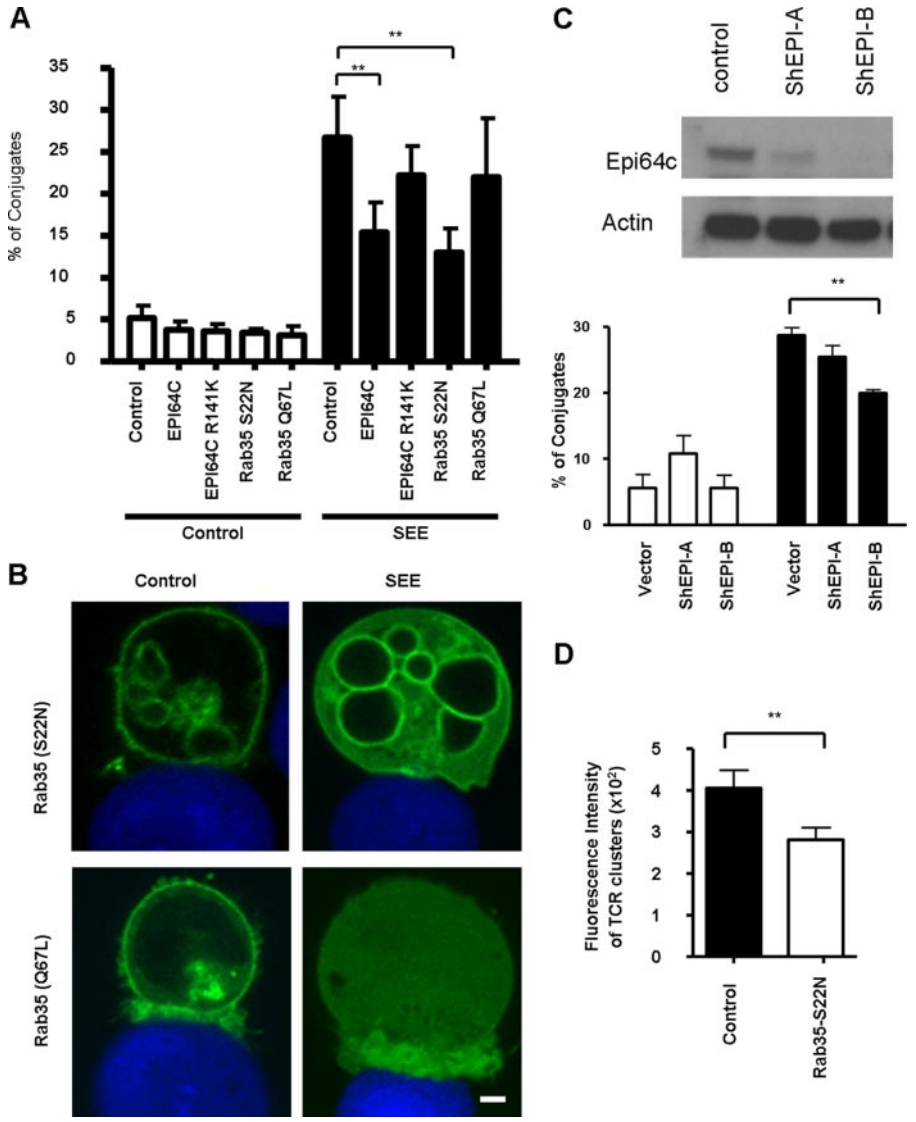

FIGURE 7. **Perturbations of Rab35 or EPI64C impair conjugate formation.** *A*, quantitation of conjugate formation between transfected Jurkat cells and Raji cells in the presence or absence of superantigen SEE assessed by flow cytometry. Labels indicate the construct with which the Jurkat cells were transfected. Values plotted are the mean ± S.E. for results from five independent experiments. **, $p < 0.015$. *B*, representative images of Jurkat cells transfected with either dominant negative GFP-Rab35 (*S22N*) or constitutively active GFP-Rab35 (*Q67L*) in physical contact with Raji cells (stained with CellTracker Blue) with or without SEE. *C*, Jurkat cells were transfected with shEPI-A and shEPI-B vectors, and lysates were immunoblotted as indicated. Quantitation is shown of conjugate formation between Jurkat cells (transfected with the indicated construct) and Raji cells in the presence or absence of superantigen SEE assessed by flow cytometry. Values plotted are the mean ± S.E. for results from three independent experiments. **, $p < 0.015$. *D*, quantitative scoring of enrichment of TCR at the IS in 25 cells from RFP- and Rab35 DN-transfected Jurkat. *Bars* represent mean ± S.E. from three independent experiments. **, difference is significant at $p = 0.01$ by the nonparametric Mann-Whitney test.

in intracellular vesicles in T cells between TCR, Rab35, and TfR. In addition to plasma membrane localization, Rab35 localizes to intracellular vesicles, especially in the pericentriolar region (Fig. 5, *A* and *B*) where there is substantial colocalization with TCR (Fig. 5*B*) and TfR (data not shown). Additional clarity is provided by images of vesicles in Rab35-DN-transfected cells that are more sharply defined, apparently because the GDP-bound form is preferentially bound to those vesicles and less abundant in cytosol. Those show particularly clear substantial colocalization of Rab35 DN with TfR (Fig. 4*B*) and TCR (Fig. 4*C*). All three of our experimental manipulations that alter normal cycling of Rab35 between GDP- and GTP-bound forms impair conjugate formation: Rab35-DN transfection (because dominant negative small G-proteins block endogenous guanine nucleotide exchange factors) (36), EPI64C transfection (where GAP function will dominate), and EPI64C knock down (where GAP function is deficient). Blocking of cycling *per se* is likely to impair function because cycling is critical for Rab localization (18, 37). The only condition that does not impair conjugate formation is transfection with Rab35-constitutive active, which would not be expected to inhibit cycling of endogenous Rab35. Given that TCR and TfR are fellow travelers in recycling endosomes (Ref. 13 and present studies) and that Rab35 regulates TfR return to the plasma membrane (Ref. 23 and present studies), our preferred model is that Rab35 and EPI64 regulate IS formation by regulating TCR transport to the IS.

The role of Rab35 in regulating membrane receptor recycling, first demonstrated by Echard in HeLa cells (23), is confirmed and extended by our studies in Jurkat cells. In both contexts, TfR externalization (a classical approach to studying recycling) is impaired by dominant negative Rab35 (and in our studies by EPI64C). A remarkable link between the TfR recycling and TCR transport was made by Alcover and coworkers, who demonstrated that these two receptors colocalize in recycling endosomes and at the IS (13). The present studies integrate the Rab35-Tfr connection in HeLa cells with the TfR-TCR connection in T cells and confirm an intimate relationship

It is worthwhile considering possible alternative interpretations of the data. First, because large vacuoles are present after Rab35DN and EPI64C transfection it is possible that the cells are globally functionally impaired. This seems unlikely because compartments such as lysosomes, ER, and early endosomes were conspicuously normal (Fig. 1*C*) and complex cellular functions (such as adhesion, migration, and overall growth) of transfected cells were indistinguishable from normal (data not shown). Second, it is conceivable that impaired conjugate formation is due to another function of Rab35 beyond its role in recycling. For example, Rab35 contributes to cytokinesis (23),

its overexpression can promote spreading (38), and our studies also suggest that Rab35 regulates processes on the cell surface also, because transfection with Rab35 wild type causes increased prominence of peripheral processes in Jurkat cells compared with transfection with two other Rab constructs (Fig. 5*A*). Such possibilities cannot be discounted but are currently hypothetical.

A promising area for future study is investigation of the molecular interactions by which Rab35 contributes to TCR transport/exocytosis. Based on the remarkable diversity of roles played by other Rabs, diverse possibilities warrant consideration, including especially regulation of vesicle transport by motor proteins and regulation of vesicle fusion (17, 18).

A key emerging concept in cell biology is that endocytic pathways and signaling pathways are intimately related (39, 40). These studies for the first time link a specific Rab and RabGAP to a central current topic of immunological investigation, the immunological synapse.

Acknowledgments—We thank Drs. Valarie Barr, Daniel D. Billadeau, Trian Chavakis, Arnaud Echard, Dom Esposito, Timothy S. Gomez, Walter Knapp, Paul Roche, Al Singer, and Even Walseng for insightful discussion and/or generous provision of reagents.

REFERENCES

1. Billadeau, D. D., Nolz, J. C., and Gomez, T. S. (2007) *Nat. Rev. Immunol.* **7,** 131–143
2. Dustin, M. L. (2005) *Semin. Immunol.* **17,** 400–410
3. Huang, Y., and Burkhardt, J. K. (2007) *J. Cell Sci.* **120,** Pt. 5, 723–730
4. Cemerski, S., and Shaw, A. (2006) *Curr. Opin. Immunol.* **18,** 298–304
5. Saito, T., and Yokosuka, T. (2006) *Curr. Opin. Immunol.* **18,** 305–313
6. Viola, A., Schroeder, S., Sakakibara, Y., and Lanzavecchia, A. (1999) *Science* **283,** 680–682
7. Stinchcombe, J. C., Bossi, G., Booth, S., and Griffiths, G. M. (2001) *Immunity* **15,** 751–761
8. Singer, S. J. (1992) *Science* **255,** 1671–1677
9. Favier, B., Burroughs, N. J., Wedderburn, L., and Valitutti, S. (2001) *Int. Immunol.* **13,** 1525–1532
10. Wulfing, C., and Davis, M. M. (1998) *Science* **282,** 2266–2269
11. Tskvitaria-Fuller, I., Rozelle, A. L., Yin, H. L., and Wulfing, C. (2003) *J. Immunol.* **171,** 2287–2295
12. Liu, H., Rhodes, M., Wiest, D. L., and Vignali, D. A. (2000) *Immunity* **5,** 665–675
13. Das, V., Nal, B., Dujeancourt, A., Thoulouze, M. I., Galli, T., Roux, P., Dautry-Varsat, A., and Alcover, A. (2004) *Immunity* **20,** 577–588
14. Arkhipov, S. N., and Maly, I. V. (2006) *Biophys. J.* **91,** 4306–4316
15. Stinchcombe, J. C., Majorovits, E., Bossi, G., Fuller, S., and Griffiths, G. M. (2006) *Nature* **443,** 462–465
16. Geisler, C. (2004) *Crit. Rev. Immunol.* **24,** 67–86
17. Jordens, I., Marsman, M., Kuijl, C., and Neefjes, J. (2005) *Traffic* **6,** 1070–1077
18. Grosshans, B. L., Ortiz, D., and Novick, P. (2006) *Proc. Natl. Acad. Sci. U. S. A.* **103,** 11821–11827
19. Pan, X., Eathiraj, S., Munson, M., and Lambright, D. G. (2006) *Nature* **442,** 303–306
20. Itoh, T., and Fukuda, M. (2006) *J. Biol. Chem.* **281,** 31823–31831
21. Reczek, D., and Bretscher, A. (2001) *J. Cell Biol.* **153,** 191–206
22. Hanono, A., Garbett, D., Reczek, D., Chambers, D. N., and Bretscher, A. (2006) *J. Cell Biol.* **175,** 803–813
23. Kouranti, I., Sachse, M., Arouche, N., Goud, B., and Echard, A. (2006) *Curr. Biol.* **16,** 1719–1725
24. Wahl, S. M., Katona, I. M., Stadler, B. M., Wilder, R. L., Helsel, W. E., and Wahl, L. M. (1984) *Cell. Immunol.* **85,** 384–395
25. Brown, M. J., Nijhara, R., Hallam, J. A., Gignac, M., Yamada, K. M., Erlandsen, S. L., Delon, J., Kruhlak, M., and Shaw, S. (2003) *Blood* **102,** 3890–3899
26. Zacharias, D. A., Violin, J. D., Newton, A. C., and Tsien, R. Y. (2002) *Science* **296,** 913–916
27. Kuroda, T. S., and Fukuda, M. (2005) *Methods Enzymol.* **403,** 431–444
28. Fukuda, M., Katayama, E., and Mikoshiba, K. (2002) *J. Biol. Chem.* **277,** 29315–29320
29. Itoh, T., Satoh, M., Kanno, E., and Fukuda, M. (2006) *Genes Cells* **11,** 1023–1037
30. Nolz, J. C., Gomez, T. S., Zhu, P., Li, S., Medeiros, R. B., Shimizu, Y., Burkhardt, J. K., Freedman, B. D., and Billadeau, D. D. (2006) *Curr. Biol.* **16,** 24–34
31. Band, A. M., Ali, H., Vartiainen, M. K., Welti, S., Lappalainen, P., Olkkonen, V. M., and Kuismanen, E. (2002) *FEBS Lett.* **531,** 513–519
32. Su, A. I., Wiltshire, T., Batalov, S., Lapp, H., Ching, K. A., Block, D., Zhang, J., Soden, R., Hayakawa, M., Kreiman, G., Cooke, M. P., Walker, J. R., and Hogenesch, J. B. (2004) *Proc. Natl. Acad. Sci. U. S. A.* **101,** 6062–6067
33. Fuchs, E., Haas, A. K., Spooner, R. A., Yoshimura, S., Lord, J. M., and Barr, F. A. (2007) *J. Cell Biol.* **177,** 1133–1143
34. Matsumoto, Y., Imai, Y., Lu Yoshida, N., Sugita, Y., Tanaka, T., Tsujimoto, G., Saito, H., and Oshida, T. (2004) *FEBS Lett.* **572,** 135–140
35. Zhang, X. M., Walsh, B., Mitchell, C. A., and Rowe, T. (2005) *Biochem. Biophys. Res. Commun.* **335,** 154–161
36. Feig, L. A. (1999) *Nat. Cell Biol.* **1,** E25–E27
37. Goody, R. S., Rak, A., and Alexandrov, K. (2005) *Cell. Mol. Life Sci.* **62,** 1657–1670
38. Heo, W. D., and Meyer, T. (2003) *Cell* **113,** 315–328
39. Polo, S., and Di Fiore, P. P. (2006) *Cell* **124,** 897–900
40. Le Roy, C., and Wrana, J. L. (2005) *Dev. Cell* **9,** 167–168